

Technical Paper

FA 10.3

A 0.9V 150MHz 10mW 4mm² 2-D Discrete Cosine Transform Core Processor with Variable-Threshold-Voltage Scheme

Tadahiro Kuroda, Tetsuya Fujita, Shinji Mita, Tetsu Nagamatu, Shinichi Yoshioka, Fumihiko Sano, Masayuki Norishima, Masayuki Murota, Makoto Kako, Masaaki Kinugawa, Masakazu Kakumu, Takayasu Sakurai

Toshiba Corp., Kawasaki, Japan

This two-dimensional 8x8 discrete cosine transform (DCT) core processor for portable multimedia equipment with HDTV-resolution in a 0.3 μ m CMOS triple-well double-metal technology operates at 150MHz from a 0.9V power supply and consumes 10mW, only 2% power dissipation of a previous 3.3V DCT [1]. Circuit techniques for dynamically varying threshold voltage reduce active power dissipation with negligible overhead in speed, standby power and chip area.

Lowering both of supply voltage, V_{DD} , and threshold voltage, V_{th} , enables high-speed low-power operation, but raises two problems: 1) degradation of worst case speed due to V_{th} fluctuation in low V_{DD} [2], 2) increase in standby power dissipation in low V_{th} [3]. The variable

Table of Contents

Paper Index

Abstract

Continued...



threshold-voltage scheme (VT scheme) in Figure 1 solves these two problems by controlling substrate bias, V_{BB} , with substrate-bias feed-back control circuits. V_{th} is controlled at 0.1V in the active mode and 0.5V in the standby mode. V_{BB} of -0.5V is applied in the active mode and -3.3V in the standby mode.

Figure 2 depicts the VT scheme block diagram. It consists of leakage current monitors (LCMs), self substrate bias (SSB) circuits, and a substrate charge injector (SCI) circuit. In the active mode, the SSB controls V_{BB} to compensate V_{th} fluctuation. In standby mode, the SSB applies deeper V_{BB} to increase V_{th} and cut off leakage. The SCI is used for fast transition from standby to active mode. Although other parts of the chip work on 0.9V V_{DD} , the VT circuit itself works on 3.3V V_{DD} that usually is available on a chip for standard interfaces with other chips.

As illustrated in Figure 3, the VT scheme uses four voltage levels for the V_{BB} control; $V_{active(+)} = -0.3V$, $V_{active} = -0.5V$, $V_{active(-)} = -0.7V$, and $V_{standby} = -3.3V$. After a power-on, the SSB begins to draw 100 μ A from the substrate to lower V_{BB} using a 50MHz ring oscillator. When V_{BB} goes lower than $V_{active(+)}$, the SSB drops to 5MHz and draws 10 μ A to control V_{BB} more precisely. The SSB stops when V_{BB} drops below $V_{active} \cdot V_{BB}$, however, rises gradually due to device leakage current through MOS

Table of Contents

Paper Index

Abstract



transistors and junctions, and reaches V_{active} to activate the SSB again. In this way, V_{BB} is controlled at V_{active} . When “SLEEP” is asserted (“1”) in the standby mode, the SCI is disabled and the SSB is activated. The SSB begins to draw 100 μ A from a substrate until V_{BB} reaches $V_{standby}$. When SLEEP=0, the SSB is disabled and the SCI is activated. The SCI injects 30mA current into the substrate until V_{BB} reaches $V_{active(-)}$. Active-to-standby mode transition takes about 100 μ s, and a standby-to-active, 0.1 μ s.

Figure 4 depicts a circuit schematic of the leakage current monitor (LCM) a key to the accurate control in the VT scheme. Transistors M1 and M2 in a bias generator operate in the subthreshold region. When an MOS transistor is in subthreshold its drain current is:

$$I_{DS} = I_0/W_0 \cdot W \cdot 10^{(V_{gs} - V_T)/S} \quad (1)$$

where S is the subthreshold swing, V_T is threshold voltage, I_0/W_0 is the current density to define V_T , and W is the channel width. By applying (1), the output voltage of the bias generator, V_b , is:

$$V_b = S \cdot \log (W_2/W_1) \quad (2)$$

where W1 and W2 is the channel width of M1 and M2, respectively. Leakage current of DCT, $I_{leak.DCT}$, and monitored leakage current, $I_{leak.LCM}$, can be calculated from (1), and a current magnification factor of LCM, X_{LCM} , can be expressed as

$$X_{LCM} = I_{leak.LCM} / I_{leak.DCT} = (W_2/W_1) \cdot (W_{LCM} / W_{DCT}) \quad (3)$$

Table of Contents

Paper Index

Abstract



where W_{DCT} is the total channel width of the DCT and W_{LCM} is the channel width of M4. This implies that X_{LCM} is determined only by the transistor size ratio and independent of the power supply voltage, temperature, and process fluctuation. Figure 5 shows simulated variation of X_{LCM} due to circuit condition changes and process fluctuation. The variation is within 15%, resulting in less than 1% error in V_{th} control. The power overhead of the monitor circuit is about 0.1% and 10% of the total power dissipation in the active and the standby mode, respectively. Transistor M3 isolates the Nout node from the N1 node and the parasitic capacitance of M4. This keeps the signal swing on N1 small to reduce delay and improve dynamic V_{th} controllability.

Area penalty induced by the VT scheme is negligible. Since the substrate current generation due to impact ionization is four orders of magnitude smaller in 0.9V V_{DD} than in 3.3V V_{DD} , the pumping current in the SSB is several per cent of that in DRAMs. Not many substrate contacts are needed. To reduce substrate noise induced by drain-substrate capacitive coupling, most of the substrate diffusions in the DCT macro are replaced by source diffusions and the rest are used for the substrate-bias separation, which imposes 0.5% area penalty.

Table of Contents

Paper Index

Abstract



In the VT scheme, no transistor sees high-voltage stress of gate oxide and junctions. Transistors are optimized for use at 3.3V. The gate oxide thickness is 8nm. The maximum voltage that assures reliability of the gate oxide is $V_{DD}+10\%$, or 3.6V. The substrate charge injector (SCI) in Figure 6 receives a control signal that swings between V_{DD} and GND at node N1 to drive substrate from $V_{standby}$ to GND. In standby-to-active transition, $V_{DD} + |V_{standby}|$ is applied between N1 and N2. $|V_{GS}|$ and $|V_{GD}|$ of M1 and M2, however, never exceeds the larger of V_{DD} and $|V_{standby}|$. All other transistors in the VT circuits and the DCT macro receive $(V_{DD} - V_{th})$ on their gate oxide when in depletion and inversion mode, and less than $|V_{standby}|$ in the accumulation mode. $V_{standby}$ should be limited to $-V_{DD}$. $V_{standby}$ of $-V_{DD}$, however, can shift V_{th} enough to reduce leakage current in standby by four orders of magnitude below that in active mode. The body effect coefficient, γ , can be adjusted independently to V_{th} in any device generations by controlling the doping concentration density in the channel-substrate depletion layer.

A chip micrograph appears in Figure 7. The VT circuits occupy $0.58 \times 0.74 \text{mm}^2$. The increase in cost and turn-around time by introducing triple-well process is less than 5%.

Table of Contents

Paper Index

Abstract



Acknowledgments:

The authors acknowledge encouragement of A. Kanuma, J. Iwamura, K. Maeguchi, O. Ozawa, and Y. Unno.

References:

[1] Matsui, M., et al. , "200MHz Video Compression Macrocells Using Low-Swing Differential Logic," ISSCC Digest of Technical Papers, pp. 76-77, Feb., 1994.

[2] Kobayashi, T., T. Sakurai, "Self-Adjusting Threshold-Voltage Scheme (SATS) for Low-Voltage High-Speed Operation," Proc. 1994 CICC, pp. 271-274, May, 1994.

[3] Seta, K., et al., "50% Active-Power Saving without Speed Degradation using Standby Power Reduction (SPR) Circuit," ISSCC Digest of Technical Papers, pp. 318-319, Feb., 1995.

Table of Contents

Paper Index

Abstract



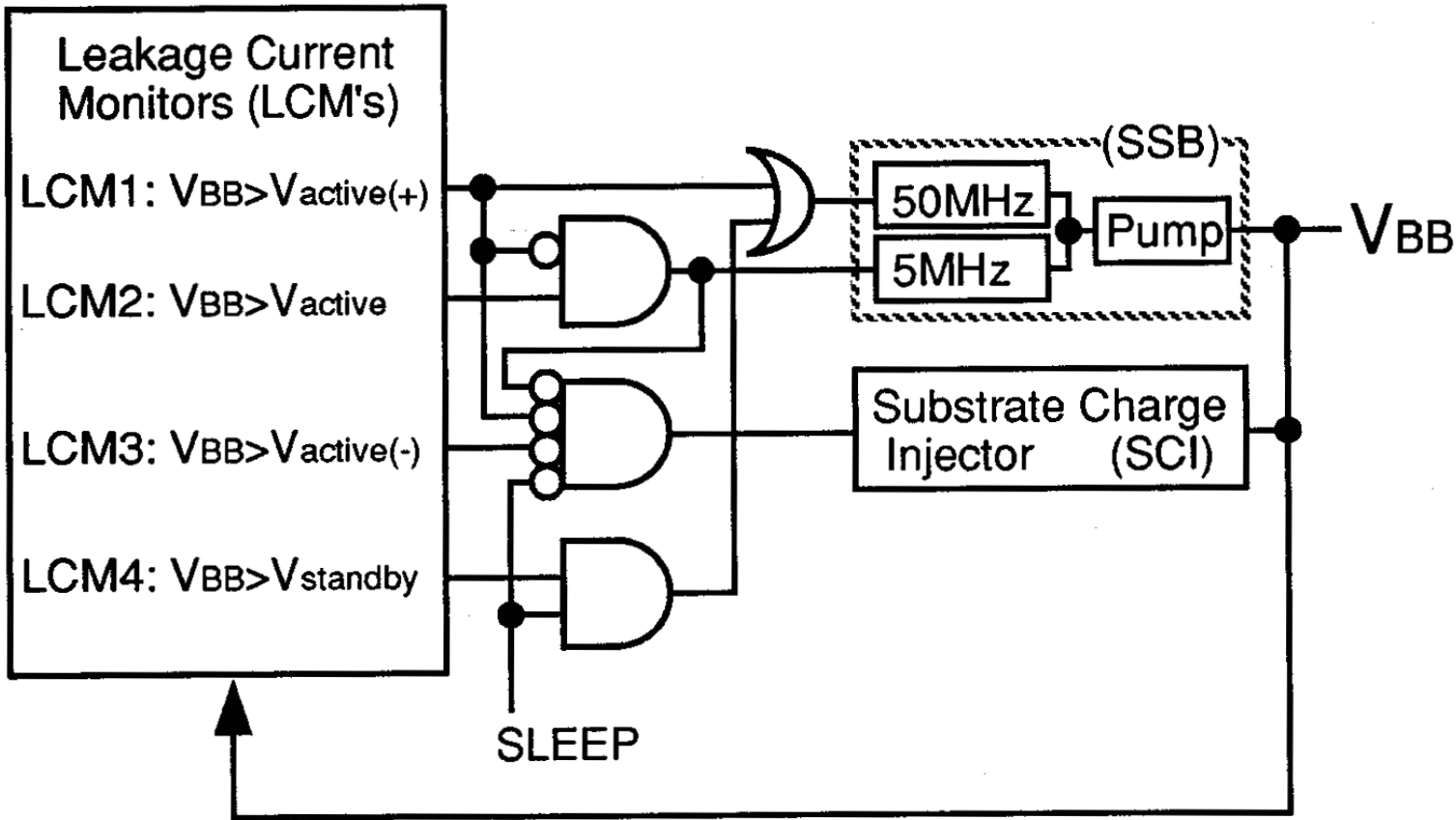


Table of Contents

Paper Index

Abstract

Figure 2: VT block diagram.

Continued...



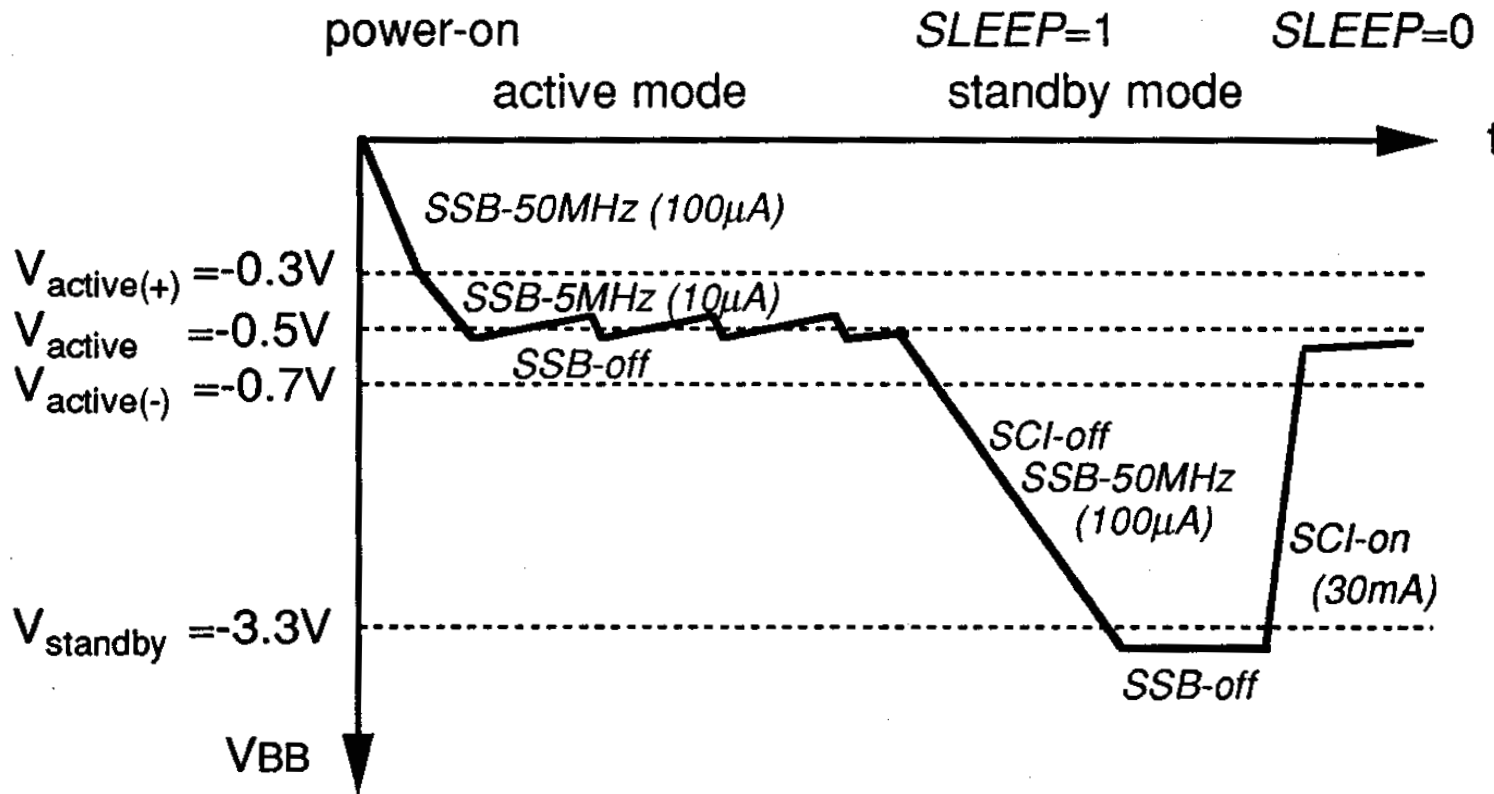


Figure 3: Substrate-bias control in VT.

Table of Contents

Paper Index

Abstract

Continued...



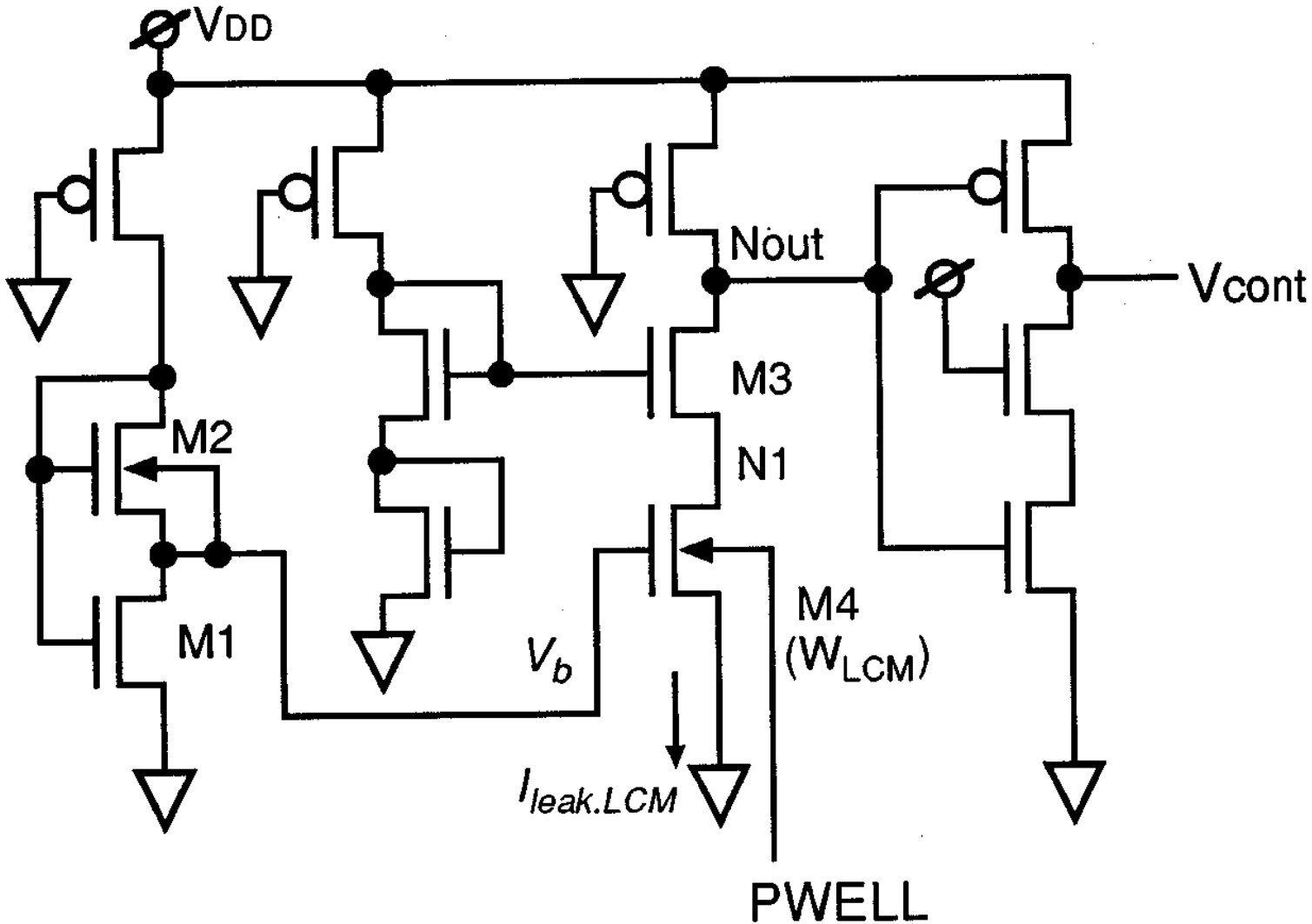


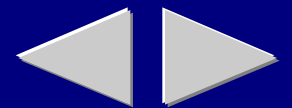
Figure 4: Leakage current monitor (LCM).

Table of Contents

Paper Index

Abstract

Continued...



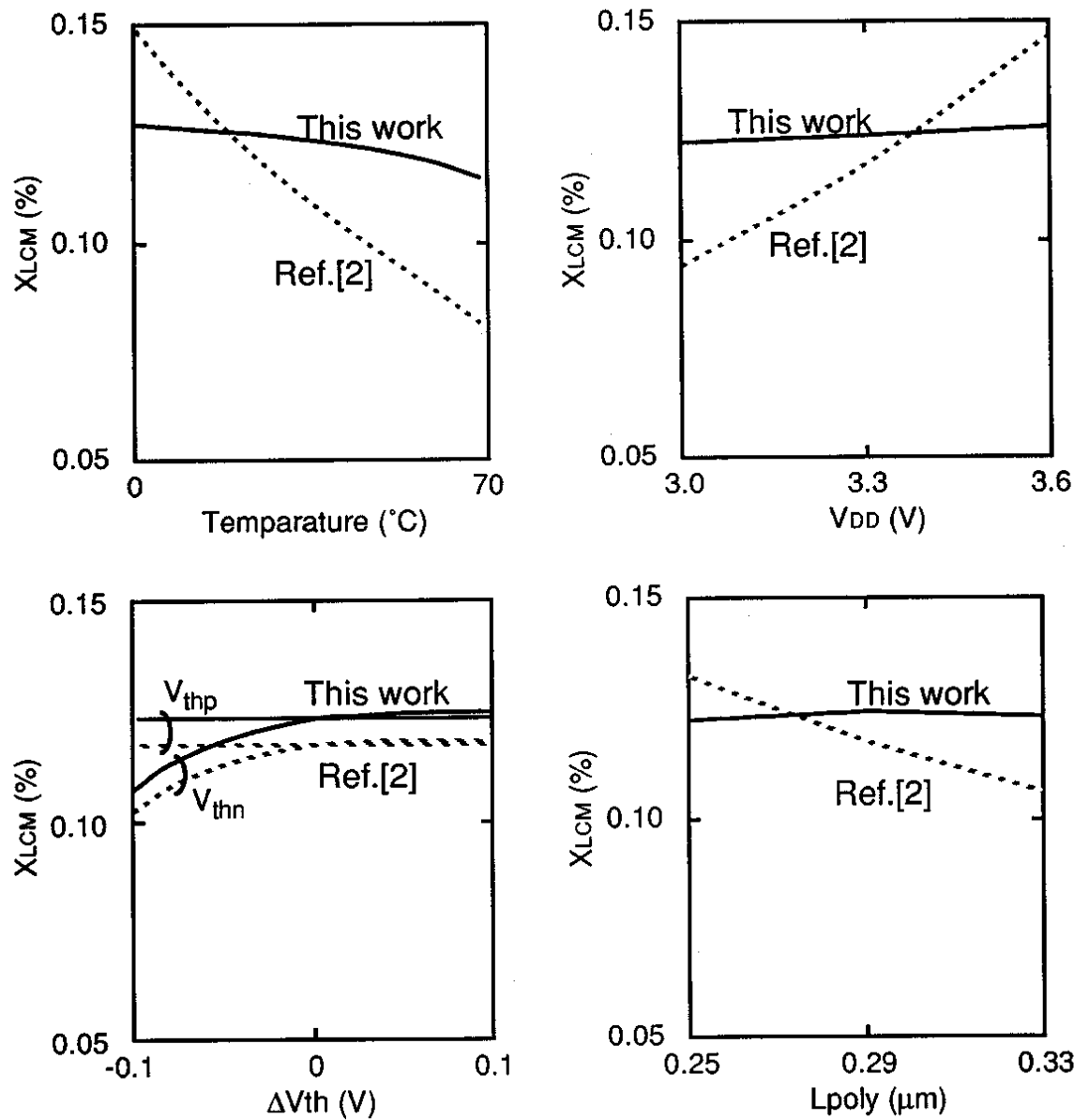


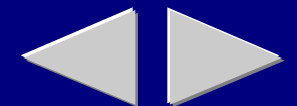
Figure 5: Current magnification factor of LCM, X_{LCM} dependence on circuit and process deviations.

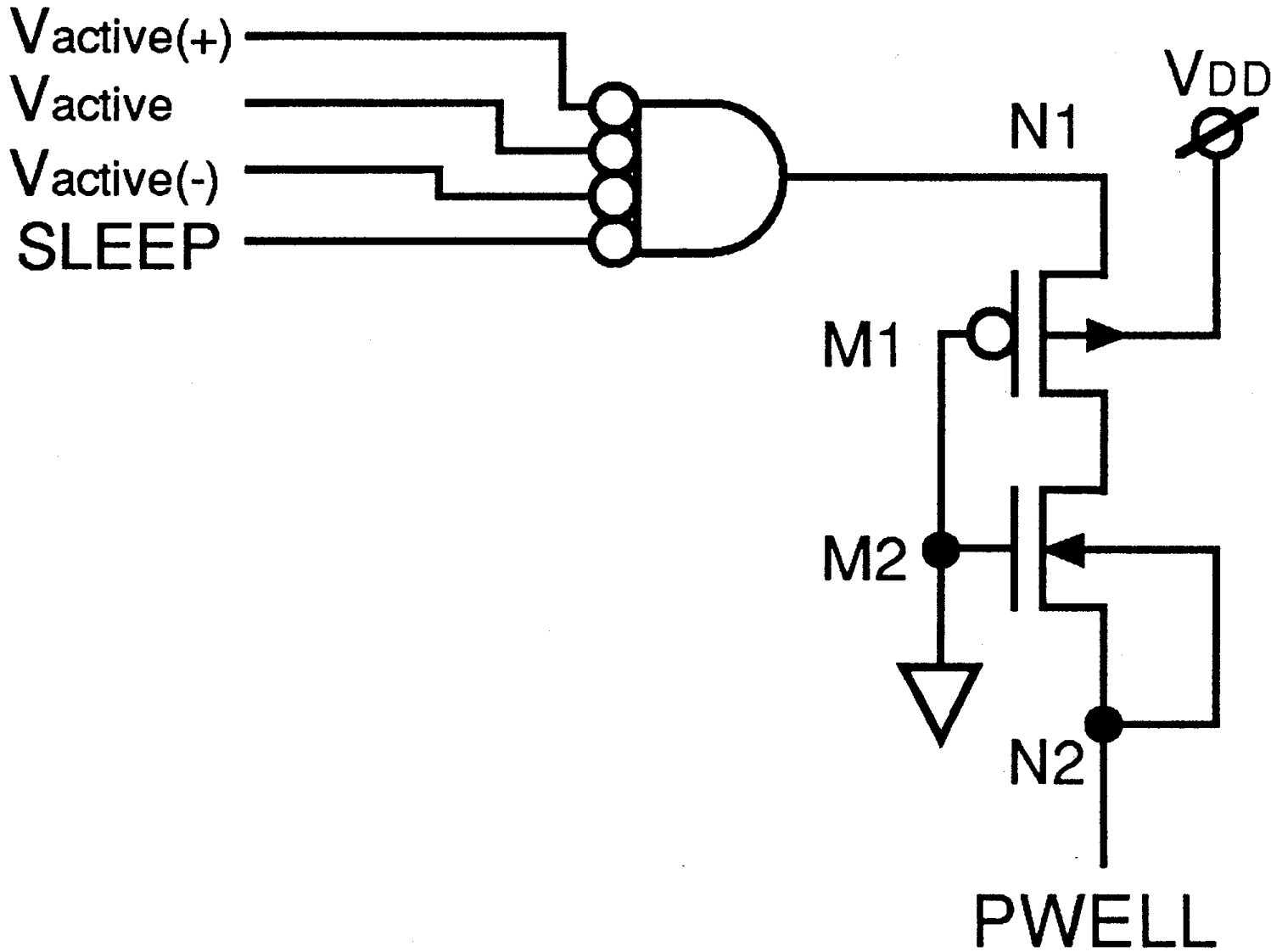
Continued...

Table of Contents

Paper Index

Abstract





[Table of Contents](#)

[Paper Index](#)

[Abstract](#)

Figure 6: Substrate charge injector (SCI).

Continued...

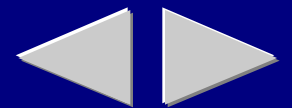


Table of Contents

Paper Index

Abstract

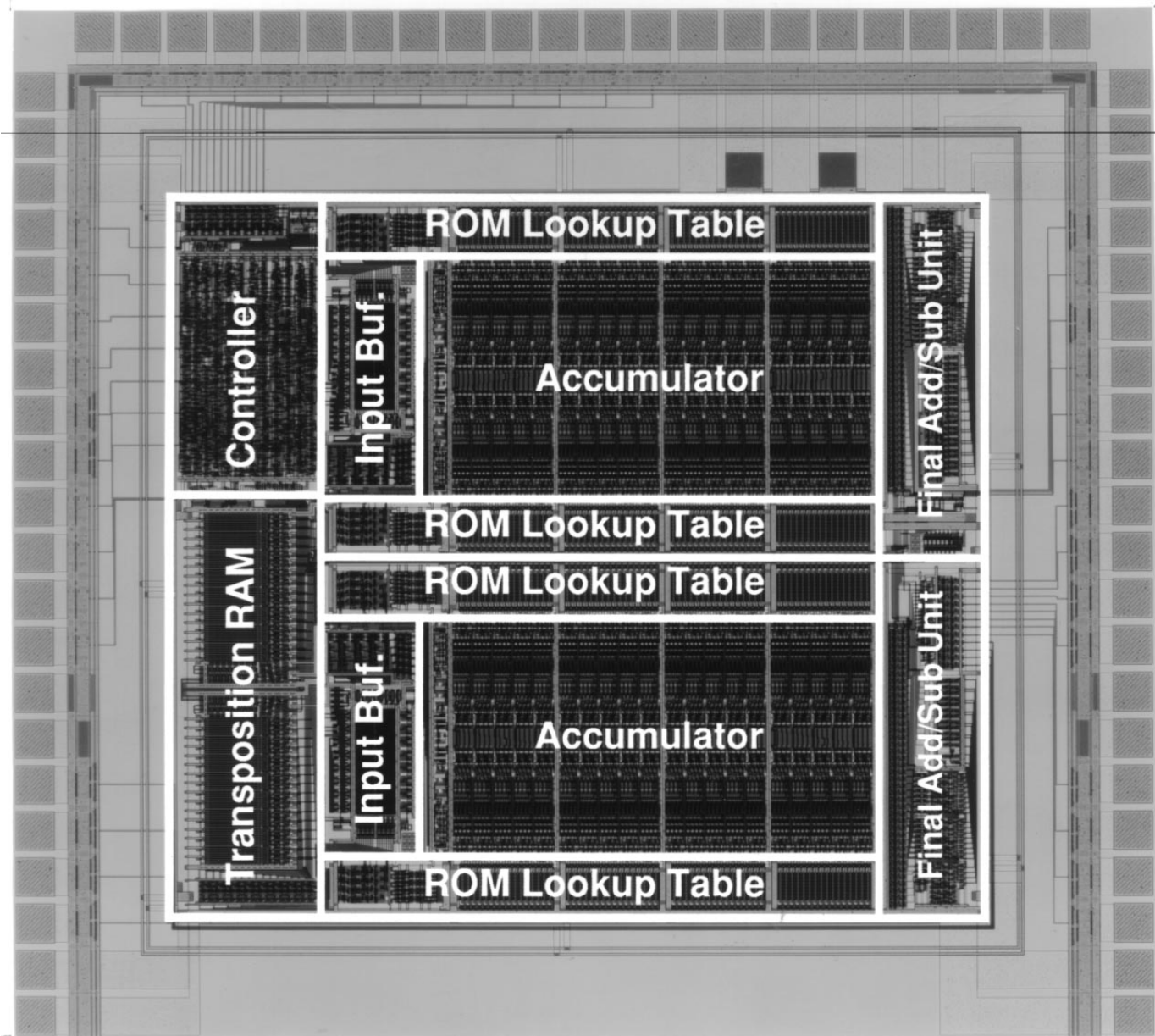


Figure 7: Chip micrograph.

Continued...

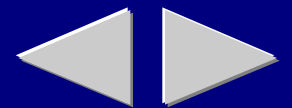




Table of Contents

Paper Index

Abstract

Source

1996 IEEE International Solid-State Circuits Conference
1996 Digest of Technical Papers, pp. 166-167.

